

Versatile Vapochromic Behavior Accompanied by a Phase Change between Charge-Polarization State and Charge-Density-Wave State in a Quasi-One-Dimensional Iodo-Bridged Dinuclear Platinum Mixed-Valence Compound, $[\{\text{NH}_3(\text{CH}_2)_5\text{NH}_3\}_2]\text{-}[\text{Pt}_2(\text{pop})_4\text{I}]\cdot 4\text{H}_2\text{O}$

Masahiro Yamashita,^{*1,4} Kouichi Takizawa,²
Satoshi Matsunaga,² Daisuke Kawakami,^{1,4}
Hiroaki Iguchi,^{1,4} Shinya Takaishi,^{1,4}
Takashi Kajiura,^{1,4} Fumiyasu Iwahori,²
Tomohiko Ishii,² Hitoshi Miyasaka,²
Ken-ichi Sugiura,² Hiroyuki Matsuzaki,³
Hideo Kishida,³ and Hiroshi Okamoto³

¹Department of Chemistry, Graduate School of Science, Tohoku University, 6-3 Aoba, Aramaki, Aoba-ku, Sendai 980-8578

²Department of Chemistry, Graduate School of Science, Tokyo Metropolitan University, 1-1 Minamiohsawa, Hachioji, Tokyo 192-0397

³Department of Advanced Materials Science, Graduate School of Frontier Science, The University of Tokyo, 515 Kashiwanoha, Kashiwa 277-8561

⁴CREST (JST), 6-3 Aoba, Aramaki, Aoba-ku, Sendai 980-8578

Received February 15, 2006; E-mail: yamasita@agnus.chem.tohoku.ac.jp

This communication describes versatile vapochromic behavior that is accompanied by a phase change between charge-polarization (CP) and charge-density-wave (CDW) states with increasing and decreasing temperature in $[\{\text{NH}_3(\text{CH}_2)_5\text{NH}_3\}_2][\text{Pt}_2(\text{pop})_4\text{I}]\cdot 4\text{H}_2\text{O}$ (pop = $\text{P}_2\text{H}_2\text{O}_5^{2-}$) (**1**).

Recently, quasi-one-dimensional halogen-bridged mixed-valence compounds (MX chains) have interesting physical properties, such as intense and dichroic intervalence charge-transfer bands, overtone progressions of resonance Raman spectra, luminescence spectra with large Stokes-shifts, large third-order nonlinear optical properties, midgap absorptions attributable to solitons and polarons, one-dimensional model compounds of high T_c copper oxide superconductors, etc.¹ Theoretically, these MX chains are considered as Peierls–

Hubbard systems, in which the electron–phonon interaction (S), the electron transfer (T), and the intra- and inter-site Coulomb repulsion energies (U and V, respectively) compete or cooperate with each other.² Pt and Pd compounds take charge-density-wave (CDW) or $\text{M}^{\text{II}}\text{–M}^{\text{IV}}$ mixed-valence states due to electron–phonon interactions (S). Therefore, these complexes are Robin–Day class II type mixed-valence compounds.³ On the other hand, Ni compounds take Ni^{III} Mott–Hubbard states due to strong electron–correlations (U). Very strong antiferromagnetic interactions are observed among the spins located on the $\text{Ni}^{\text{III}}d_{z^2}$ orbital through the p_z orbitals of bridging halogenide ions in these compounds.⁴ Therefore, the Ni complexes are Robin–Day class III type compounds. Recently, a gigantic third-order nonlinear optical susceptibility ($\approx 10^{-4}$ esu) was observed for $[\text{Ni}^{\text{III}}(\text{chxn})_2\text{Br}]\text{Br}_2$ (chxn = 1*R*,2*R*-diaminocyclohexane).⁵

As an extension to MX chain systems, quasi-one-dimensional halogen-bridged dinuclear Pt complexes (MMX chains) have been reported.^{6,7} Theoretically, the mixed valency of the MMX chain system that have a formal oxidation state of $\text{Pt}^{\text{II}}\text{Pt}^{\text{III}}$ can be classified into the following four groups and is also known to be strongly correlated to the position of the bridging halogenide ion.

- (a) $\text{–Pt}^{2.5+}\text{–Pt}^{2.5+}\text{–X–Pt}^{2.5+}\text{–Pt}^{2.5+}\text{–X–}$
(average-valence (AV) state)
- (b) $\text{…Pt}^{2+}\text{–Pt}^{2+}\text{…X–Pt}^{3+}\text{–Pt}^{3+}\text{–X…}$
(charge-density-wave (CDW) state)
- (c) $\text{…Pt}^{2+}\text{–Pt}^{3+}\text{–X…Pt}^{2+}\text{–Pt}^{3+}\text{–X…}$
(charge-polarization (CP) state)
- (d) $\text{…Pt}^{2+}\text{–Pt}^{3+}\text{–X–Pt}^{3+}\text{–Pt}^{2+}\text{…X…}$
(alternating charge-polarization (ACP) state)

So far, two types of the MMX chains have been reported, namely a dta-system⁶ and a pop-system.⁷ In the former compounds, Pt–Pt dimer units are coordinated by four dithioacetate (dta) derivatives, forming a lantern structure, and these units are bridged by iodide ions to form neutral chains. The latter compounds have chemical formulas of $\text{A}_4[\text{Pt}_2(\text{pop})_4\text{X}]\cdot n\text{H}_2\text{O}$ or $\text{A}_2'[\text{Pt}_2(\text{pop})_4\text{X}]\cdot n\text{H}_2\text{O}$ (pop = $\text{P}_2\text{H}_2\text{O}_5^{2-}$; A = K, Na, Li, Cs, Rb, alkyl ammonium, etc.; A' = alkyldiammonium; X = Cl, Br, and I). We have synthesized more than 50 compounds by substituting the cations and bridging halogens. Since the I-bridged compounds have a large hybridization between the p orbitals of bridging iodide ions and the d orbitals of platinum ions, various oxidation states are stabilized. Actually, the oxidation states of the iodo-bridged MMX compounds depend on the inter-dimer Pt…Pt distances at the Pt–I–Pt geometry, i.e., the compounds with the shortest, middle, and the longest Pt…Pt (inter-dimer) distances belong to the AV, CDW, and CP states, respectively. Recently, we have reported a pressure and photo-induced phase change between the CP and CDW states in $[\{(\text{C}_2\text{H}_5)_2\text{NH}_3\}_4][\text{Pt}_2(\text{pop})_4\text{I}]\cdot 4\text{H}_2\text{O}$.⁸ More recently, we have reported vapochromic behavior that is accompanied by a phase change between CP and CDW with increasing and decreasing temperatures in $[\{\text{NH}_3(\text{CH}_2)_4\text{NH}_3\}_2][\text{Pt}_2(\text{pop})_4\text{I}]\cdot 4\text{H}_2\text{O}$.⁹ In order for the dehydrated state (CDW state) to return to the hydrated state (CP state) by decreasing the temperature, enough humidity is needed or sometimes, the compound must

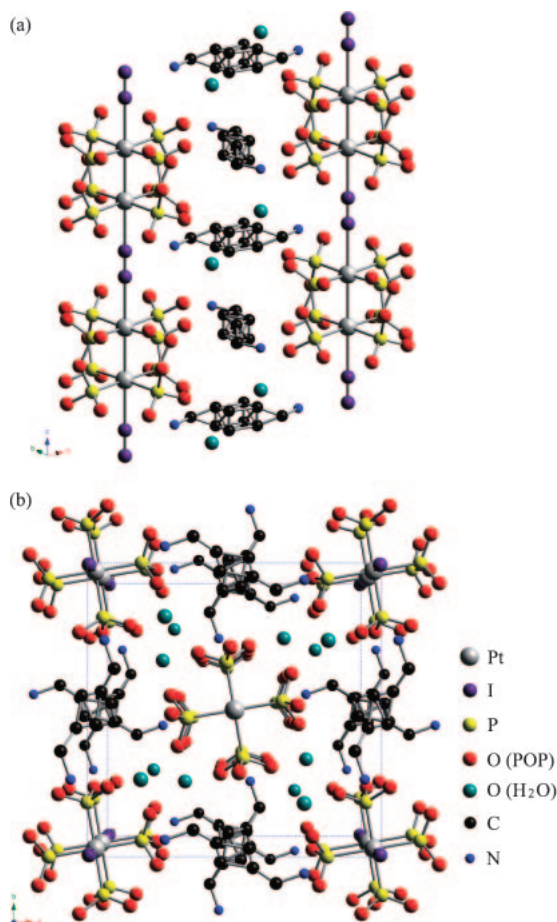


Fig. 1. Perspective views of the 3D packing of **1**. H atoms have been omitted for clarity.

be dipped into water. In this paper, we report more versatile vapochromic behavior that is accompanied by a phase change between CP and CDW states in **1**, which has a larger cation.

Different views of the crystal structure, which was determined at 297 K, are shown in Fig. 1. Two Pt atoms are linked by four pop ligands to form a lantern-type $[\text{Pt}_2(\text{pop})_4]$ unit. The two neighboring $[\text{Pt}_2(\text{pop})_4]$ units are bridged by iodide ions, forming a Pt–Pt–I linear-chain structure along the *c*-axis. The bridging iodide ions are disordered with half occupancies at the distorted positions from the midpoints between neighboring Pt dinuclear units, which suggests that this compound is in either the CP or CDW state. However, it is difficult to distinguish from X-ray structure analysis whether the ground state of this compound is the CP state or CDW state, because the displacement of iodide ions is not three-dimensionally ordered. The Pt–Pt distance is 2.838 Å, which is intermediate between the $\text{K}_4[\text{Pt}^{\text{II}}_2(\text{pop})_4] \cdot 2\text{H}_2\text{O}$ (2.925 Å)^{10a} and $\text{K}_4[\text{Pt}^{\text{III}}_2(\text{pop})_4\text{I}_2]$ (2.755 Å).^{10b} The shorter and longer Pt–I distances are 2.732 and 4.126 Å, respectively. In comparison with $[\{\text{NH}_3(\text{CH}_2)_4\text{NH}_3\}_2][\text{Pt}_2(\text{pop})_4\text{I}] \cdot 4\text{H}_2\text{O}$, the selected interatom distances relevant to their electronic states are listed in Table 1. The electronic structure of the MMX chain system strongly depends upon the Pt...Pt distance of the Pt–I–Pt geometry.⁸ In this compound, this distance is 6.858 Å, which suggests that this compound at 297 K is in the CP state, i.e., $\text{Pt}^{\text{II}}\text{–Pt}^{\text{III}}\text{–I}\cdots\text{Pt}^{\text{II}}\text{–Pt}^{\text{III}}\text{–I}$. The counter cations $\text{NH}_3(\text{CH}_2)_5\text{NH}_3^{2+}$ are surrounded by

Table 1. Comparison of the Interatomic Distances along Chains (Å)

| | A' | Pt–Pt | Pt–I | Pt...I | Pt–I–Pt |
|--|----|-----------|----------|----------|---------|
| $\text{NH}_3(\text{CH}_2)_4\text{NH}_3^{2+}$ | | 2.8374(9) | 2.722(2) | 4.249(2) | 6.971 |
| $\text{NH}_3(\text{CH}_2)_5\text{NH}_3^{2+}$ | | 2.838(1) | 2.732(2) | 4.126(2) | 6.858 |

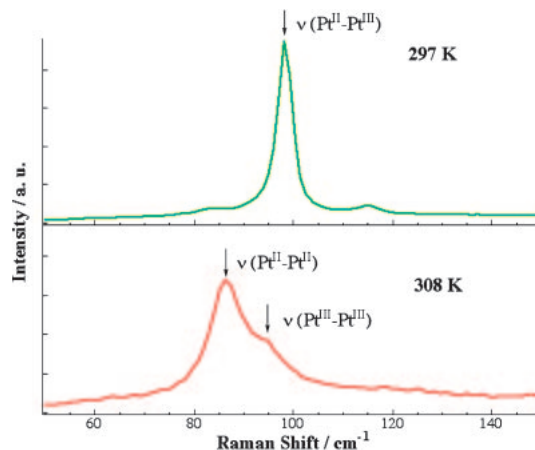


Fig. 2. Polarized Raman spectra for the polarization of $z(x,x)z(x \parallel c\text{-axis})$ at 297 and 308 K.

four Pt chains and hydrogen bonded to the pop ligands. Four H_2O molecules are also located in the inter-chain spaces.

Raman spectroscopy is a useful method to determine the oxidation states of these compounds because the CP and CDW states afford a singlet ($\nu(\text{Pt}^{\text{II}}\text{–Pt}^{\text{III}})$) and doublet ($\nu(\text{Pt}^{\text{II}}\text{–Pt}^{\text{II}})$ and $\nu(\text{Pt}^{\text{III}}\text{–Pt}^{\text{III}})$) stretching modes, respectively. Figure 2 shows the polarized Raman spectra of **1** in ambient humidity at 297 and 308 K. At 297 K, a singlet Raman peak is observed at 98 cm^{-1} . This peak is attributed to the $\text{Pt}^{\text{II}}\text{–Pt}^{\text{III}}$ stretching mode. A weak peak is also observed at 114.5 cm^{-1} , which is attributed to the $\text{Pt}^{\text{III}}\text{–I}$ stretching mode. Therefore, the ground state of this compound at 297 K is determined to be the CP state, which is consistent with that predicted from the phase diagram based on the Pt...Pt distances at the Pt–I–Pt geometry. At 308 K, on the other hand, the main signals consist of two components, which are assigned to the stretching modes of the $\text{Pt}^{\text{II}}\text{–Pt}^{\text{II}}$ (86.4 cm^{-1}) and $\text{Pt}^{\text{III}}\text{–Pt}^{\text{III}}$ (93.9 cm^{-1}). Therefore, the oxidation state of **1** at 308 K is assigned as the CDW state.

Because there is a marked color change in the crystal upon the CP-to-CDW phase change, polarized reflectivity spectra were measured. Figures 3a and 3b show the polarized reflectivity spectra and optical conductivity spectra, which were obtained by Kramers–Kronig transformation of the reflectivity spectra, respectively, at 297 and 308 K. In the optical conductivity spectrum at 297 K, an intense peak is observed at 2.24 eV. Yamamoto has theoretically showed that the lowest CT band in the CP phase can be assigned to intra-dimer CT transition.¹¹ Therefore, this peak is assigned to intra-dimer CT transition.

Upon increasing the temperature, the color of the single-crystal discontinuously changed from lustrous yellow to red (Fig. 3, insets). In the optical conductivity spectrum obtained at 308 K, an intense band is observed at 1.14 eV. Because the compounds, for which a CT band is observed between 1.0 and

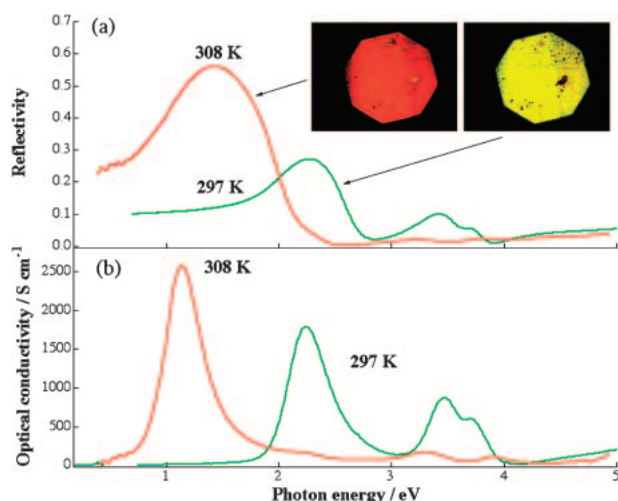


Fig. 3. (a) Polarized reflectivity and (b) optical conductivity spectra with polarization of light parallel to the *c*-axis in **1** at 297 and 308 K. The insets in (a) show the corresponding microscope images for the single crystal taken in reflection mode.

1.5 eV usually, are in a CDW state, the electronic state of **1** is assigned to the CDW state, which is consistent with the result from Raman spectroscopy. Therefore, this band is attributed to the inter-dimer transition from Pt^{II} to Pt^{III} species through the bridging iodide anions.

In order to determine the mechanism for the phase change, we performed a thermogravimetric analysis (TGA). At 350 K, the compound lost 4.91% weight, which corresponds to four H₂O molecules per formula unit (5.25%). Furthermore, from the phase diagram in Fig. S2, it is expected that the Pt–I–Pt distance decreased to ca. 6.0 Å in the dehydrated state ($E_{CT} = 1.14$ eV). Yamamoto theoretically determined that decreasing the Pt–I–Pt distance stabilizes the CDW state, which is consistent with the phase diagram and Raman spectroscopy. Therefore, vapochromic behavior is accompanied by a phase change between CP and CDW states similar to $[\{NH_3(CH_2)_4NH_3\}_2][Pt_2(pop)_4I] \cdot 4H_2O$.⁹ Single-crystal X-ray structure determination at 350 K was unsuccessful. Therefore, X-ray powder diffraction measurements were made both at 297 and 350 K. The X-ray powder pattern at 350 K is different from that at 297 K. In other words, the crystal structure at 350 K is different from that at 297 K. The vapochromic behavior in **1** occurred easily just by varying temperature in the atmosphere repeatedly, while that in $[\{NH_3(CH_2)_4NH_3\}_2][Pt_2(pop)_4I] \cdot 4H_2O$ occurred under saturated humidity atmosphere, in water, when changing from dehydrated state to hydrated state. The more versatile vapochromic behavior of the complex compared to that for $[\{NH_3(CH_2)_4NH_3\}_2][Pt_2(pop)_4I] \cdot 4H_2O$ is reasonably explained by considering the difference in the inter-chain spaces (**1**, $6.8 \text{ \AA} \times 1.7 \text{ \AA}$; $[\{NH_3(CH_2)_4NH_3\}_2][Pt_2(pop)_4I] \cdot 4H_2O$, $3.3 \text{ \AA} \times 1.6 \text{ \AA}$). Also, the cell volume of **1** ($1850.5(8) \text{ \AA}^3$) is larger than that of $[\{NH_3(CH_2)_4NH_3\}_2][Pt_2(pop)_4I] \cdot 4H_2O$ ($1747.5(2) \text{ \AA}^3$).

This work was partly supported by a Grant-in-Aid for Creative Scientific Research from the Ministry of Education, Culture, Sports, Science and Technology.

Supporting Information

Experimental details, crystallographic information file (CIF), TGA result, and XRD patterns of **1**. This material is available free of charge on the web at: <http://www.csj.jp/journals/bcsj/>.

References

- 1 a) J. S. Miller, *Extended Linear Chain Compounds*, New York and London, **1982**, Vols. I–III. b) A. R. Bishop, B. I. Swanson, *Los Alamos Sci.* **1993**, 21, 133. c) R. J. H. Clark, *Adv. Infrared Raman Spectrosc.* **1983**, 11, 95. d) G. C. Papavassiliou, A. D. J. Zdesis, *J. Chem. Soc., Faraday Trans. 2* **1980**, 76, 104. e) H. Tanino, K. Kobayashi, *J. Phys. Soc. Jpn.* **1983**, 52, 1446. f) N. Kuroda, M. Sakai, Y. Nishina, M. Tanaka, S. Kurita, *Phys. Rev. Lett.* **1987**, 58, 2122. g) Y. Iwasa, E. Funatsu, T. Hasegawa, T. Koda, M. Yamashita, *Appl. Phys. Lett.* **1991**, 59, 2219. h) R. J. Donohoe, L. A. Worl, C. A. Arrington, A. Bulou, B. I. Swanson, *Phys. Rev. B* **1992**, 45, 13185. i) H. Okamoto, Y. Kaga, Y. Shimada, Y. Oka, Y. Iwasa, T. Mitani, M. Yamashita, *Phys. Rev. Lett.* **1998**, 80, 861. j) S. Takaishi, H. Miyasaka, K. Sugiura, M. Yamashita, H. Matsuzaki, H. Kishida, H. Okamoto, H. Tanaka, K. Marumoto, H. Ito, S. Kuroda, T. Takami, *Angew. Chem., Int. Ed.* **2004**, 43, 3171.
- 2 D. Baeriswyl, A. R. Bishop, *J. Phys. C: Solid State Phys.* **1988**, 21, 339; A. Mishima, K. Nasu, *Phys. Rev. B: Condens. Matter* **1989**, 39, 5758.
- 3 M. B. Robin, P. Day, *Adv. Inorg. Radiochem.* **1967**, 9, 247.
- 4 a) K. Toriumi, Y. Wada, T. Mitani, S. Bandow, M. Yamashita, Y. Fujii, *J. Am. Chem. Soc.* **1989**, 111, 2341. b) H. Okamoto, K. Toriumi, T. Mitani, M. Yamashita, *Phys. Rev. B* **1990**, 42, 10381.
- 5 H. Kishida, H. Matsuzaki, H. Okamoto, T. Manabe, M. Yamashita, Y. Taguchi, Y. Tokura, *Nature* **2000**, 405, 929.
- 6 a) C. Bellito, A. Flamini, L. Gastaldi, L. Scaramuzza, *Inorg. Chem.* **1983**, 22, 444. b) H. Kitagawa, N. Onodera, J. Ahn, T. Mitani, M. Kim, Y. Ozawa, K. Toriumi, K. Yasui, T. Manabe, M. Yamashita, *Mol. Cryst. Liq. Cryst.* **1996**, 285, 311.
- 7 a) C.-M. Che, F. H. Herstein, W. P. Schaefer, R. E. Marsch, H. B. Gray, *J. Am. Chem. Soc.* **1983**, 105, 4604. b) M. Kurmoo, R. J. H. Clark, *Inorg. Chem.* **1985**, 24, 4420.
- 8 H. Matsuzaki, T. Matsuoka, H. Kishida, K. Takizawa, H. Miyasaka, K. Sugiura, M. Yamashita, H. Okamoto, *Phys. Rev. Lett.* **2003**, 90, 046401.
- 9 H. Matsuzaki, H. Kishida, H. Okamoto, K. Takizawa, S. Matsunaga, S. Takaishi, H. Miyasaka, K. Sugiura, M. Yamashita, *Angew. Chem., Int. Ed.* **2005**, 44, 3240.
- 10 a) M. A. Filomena Dos Remedios Pinto, P. J. Sadler, S. Neidle, M. R. Sanderson, A. Subbiah, R. Kuroda, *J. Chem. Soc., Chem. Commun.* **1980**, 13. b) K. A. Alexander, S. A. Bryan, F. R. Fronczek, W. C. Fultz, A. L. Rheingold, D. M. Roundhill, P. Stein, S. F. Watkins, *Inorg. Chem.* **1985**, 24, 2803.
- 11 S. Yamamoto, *Phys. Rev. B* **2001**, 64, 140102.